

# FROM UPC TO SEMI-CENTRAL HEAVY-ION COLLISIONS

Mariola Klusek-Gawenda

The Henryk Niewodniczański Institute of Nuclear Physics Polish Academy of Sciences

- ✓ M. K-G, P. Lebiedowicz and A. Szczurek, *Light-by-light scattering in ultraperipheral Pb-Pb collisions at energies available at the CERN Large Hadron Collider*, Phys. Rev. **C93** (2016) 044907,
- ✓ M. K-G, W. Schäfer and A. Szczurek, *Two-gluon exchange contribution to elastic  $\gamma\gamma \rightarrow \gamma\gamma$  scattering and production of two-photons in ultraperipheral ultrarelativistic heavy-ion and proton-proton collisions*, Phys. Lett. **B761** (2016) 399,
- ✓ M. K-G, R. McNulty, R. Schicker and A. Szczurek, *Light-by-light scattering in ultraperipheral heavy-ion collisions at low diphoton masses*, Phys. Rev. **D99** (2019) 9, 093013,
- ✓ Z. Citron, M. K-G et al., *Future physics opportunities for high-density QCD at the LHC with heavy-ion and proton beams*, CERN Yellow Rep. Monogr. 7 (2019) 1159-1410,
- ✓ G.K. Krintiras, I. Grabowska-Bold, M. K-G, É. Chapon, R. Chudasama, and R. Granier de Cassagnac, *Light-by-light scattering cross-section measurements at LHC*, arXiv:2204.02845 [hep-ph],  $\eta_b(1S)$ ,
- ✓ M. K-G, A. Szczurek, *Double scattering production of two positron-electron pairs in ultraperipheral heavy-ion collisions*, Phys. Lett. **B763** (2016) 416-421;
- ✓ A. van Hameren, M. K-G, A. Szczurek, *Single- and double-scattering production of four muons in ultraperipheral PbPb collisions at the Large Hadron Collider*, Phys. Lett. **B776** (2018) 84-90;
- ✓ M. K-G. Rapp, W. Schäfer, A. Szczurek, *Dilepton Radiation in Heavy-Ion Collisions at Small Transverse Momentum*, Phys. Lett. **B790** (2019) 339–344;
- ✓ M. K-G, W. Schäfer, A. Szczurek, *Centrality dependence of dilepton production via  $\gamma\gamma$  processes from Wigner distributions of photons in nuclei*, Phys. Lett. **B814** (2021) 136114;
- ✓ M. K-G, A. Szczurek, *Photoproduction of  $J/\psi$  mesons in peripheral and semicentral heavy ion collisions*, Phys. Rev. **C93** (2016) 044912.

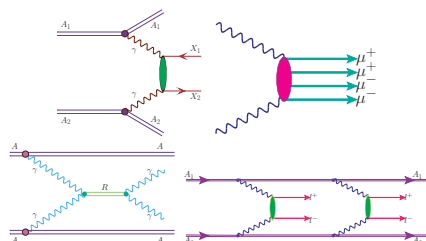
# CLASSIFICATION

## 1 Collision energy:

- low energy processes:  
 $\sqrt{s_{NN}} < 10$  MeV/nucleon;
- intermediate energies:  
 $\sqrt{s_{NN}} = (10 - 100)$  MeV/nucleon;
- relativistic energies:  
 $\sqrt{s_{NN}} = (0.1 - 100)$  GeV/nucleon;
- ultrarelativistic energies:  
 $\sqrt{s_{NN}} > 100$  GeV/nucleon;

## 3 Type of production:

### $\gamma\gamma$ fusion



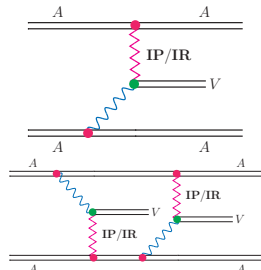
- ✓  $\rho^0 \rho^0, J/\psi J/\psi$
- ✓  $\pi^+ \pi^-, \pi^0 \pi^0$
- ✓  $c\bar{c}, b\bar{b}$
- ✓  $e^+ e^-, \mu^+ \mu^-, \tau^+ \tau^-$
- ✓  $\gamma\gamma$

## 2 Centrality (for $^{208}\text{Pb}$ ):

- central collisions:  $b \approx (0 \text{ fm} + \Delta b)$ ;
- semi-central collisions:  $b \approx (5 - 10) \text{ fm}$ ;
- semi-peripheral collisions:  $b \approx (10 - 12) \text{ fm}$ ;
- peripheral collisions:  $b \approx (12 \text{ fm} - (R_1 + R_2))$ ;
- **ultraperipheral** collisions:  $b > (R_1 + R_2)$ ;

where  $R = R_0 A^{1/3}$ .

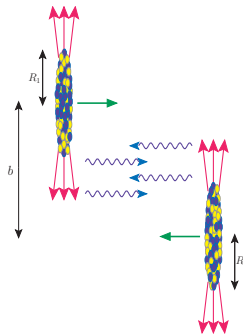
### Photoproduction



- ✓  $p\bar{p}$
- ✓  $\pi^+ \pi^- \pi^+ \pi^-$
- ✓  $e^+ e^- e^+ e^-$
- ✓  $\mu^+ \mu^- \mu^+ \mu^-$

- ✓  $\rho^0, J/\psi$
- ✓  $\rho^0 \rho^0, J/\psi J/\psi$

# EQUIVALENT PHOTON APPROXIMATION

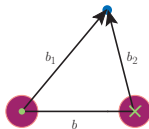


The strong electromagnetic field is a source of photons that can induce electromagnetic reactions in ion-ion collisions. Electromagnetism is a long-range force, so electromagnetic interactions occur even at relatively large ion-ion separations.

$$\text{Photon energy: } \omega = \frac{\gamma}{b} \approx \gamma \times 15 \text{ MeV}$$

$$\text{Virtuality: } Q^2 = \frac{1}{R^2} \approx 0.0008 \text{ GeV}^2$$

$$\begin{aligned} \sigma_{A_1 A_2 \rightarrow A_1 A_2 X_1 X_2} &= \int \sigma_{\gamma\gamma \rightarrow X_1 X_2} (W_{\gamma\gamma}) N(\omega_1, \mathbf{b}_1) N(\omega_2, \mathbf{b}_2) S_{abs}^2(\mathbf{b}) \frac{W_{\gamma\gamma}}{2} dW_{\gamma\gamma} dY_{X_1 X_2} d\bar{b}_x d\bar{b}_y d^2b \\ &= \int \frac{d\sigma_{\gamma\gamma \rightarrow X_1 X_2} (W_{\gamma\gamma})}{d\cos\theta} N(\omega_1, \mathbf{b}_1) N(\omega_2, \mathbf{b}_2) S_{abs}^2(\mathbf{b}) \frac{W_{\gamma\gamma}}{2} dW_{\gamma\gamma} dY_{X_1 X_2} d\bar{b}_x d\bar{b}_y d^2b \\ &\times \frac{d\cos\theta}{dy_{X_1} dy_{X_2} dp_t} \times dy_{X_1} dy_{X_2} dp_t . \end{aligned}$$



# EQUIVALENT PHOTON FLUX VS. FORM FACTOR

$$N(\omega, b) = \frac{Z^2 \alpha_{em}}{\pi^2 \beta^2} \frac{1}{\omega} \frac{1}{b^2} \times \left| \int d\chi \chi^2 \frac{F\left(\frac{\chi^2 + u^2}{b^2}\right)}{\chi^2 + u^2} J_1(\chi) \right|^2$$

$$\beta = \frac{p}{E}, \gamma = \frac{1}{\sqrt{1-\beta^2}}, u = \frac{\omega b}{\gamma \beta}, \chi = k_\perp b$$

- point-like  $F(q^2) = 1$

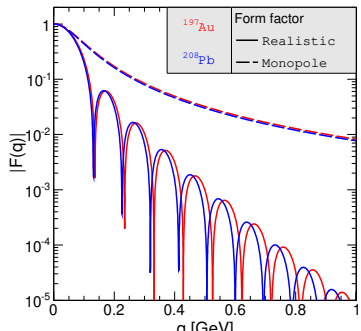
$$N(\omega, b) = \frac{Z^2 \alpha_{em}}{\pi^2 \beta^2} \frac{1}{\omega} \frac{1}{b^2} \times u^2 \left[ K_1^2(u) + \frac{1}{\gamma^2} K_0^2(u) \right]$$

- monopole  $F(q^2) = \frac{\Lambda^2}{\Lambda^2 + |\mathbf{q}|^2}$

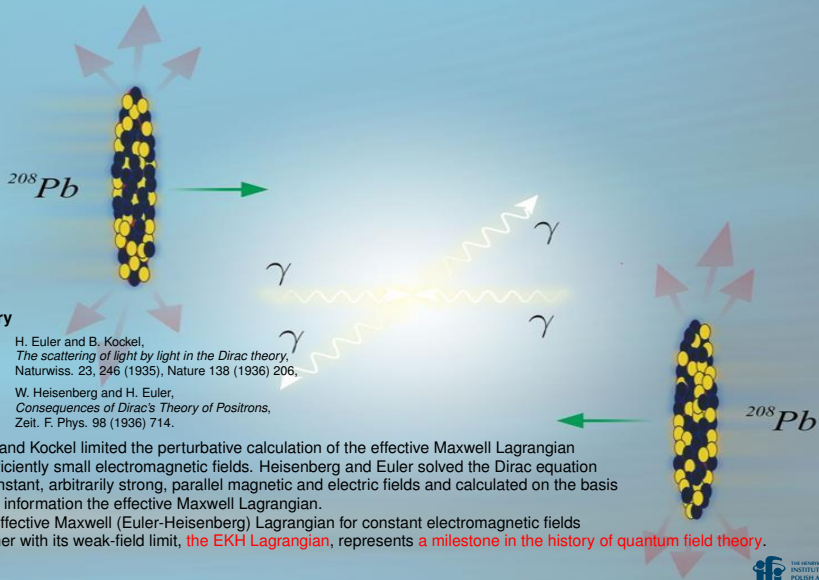
$$\sqrt{\langle r^2 \rangle} = \sqrt{\frac{6}{\Lambda^2}} = 1 \text{ fm } A^{1/3}$$

- realistic

$$F(q^2) = \frac{4\pi}{|\mathbf{q}|} \int \rho(r) \sin(|\mathbf{q}|r) r dr$$

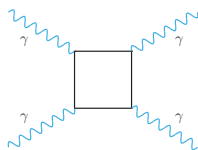


# LIGHT-BY-LIGHT SCATTERING



# LIGHT-BY-LIGHT SCATTERING

- Maxwell classical theory
  - ✓ light doesn't interact with each other
- Quantum theory
  - ✓ interaction of photons through quantum fluctuations



- $\sigma(\gamma\gamma \rightarrow \gamma\gamma) \propto \alpha_{em}^4$

→ very small

- Photon beams

✗ High-power lasers

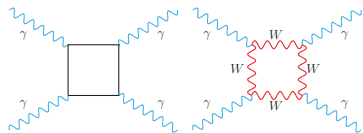
- K. Homma, K. Matsuura, K. Nakajima,  
PTEP 2016 (2016) 013C01  
*Testing helicity-dependent  $\gamma\gamma \rightarrow \gamma\gamma$  scattering in the region of MeV*

- ✓ Ultrarelativistic heavy-ion collision

- Cross section  $\propto Z^4$
- Quasi-real photons

**Boxes**

**WELL-KNOWN**



Fermionic boxes (LO QED)

FormCalc.

$$|\mathcal{M}_{\gamma\gamma \rightarrow \gamma\gamma}|^2 = \alpha_{em}^4 f(\hat{t}, \hat{u}, \hat{s})$$

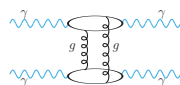
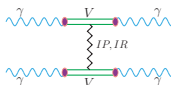
**W Box**

LoopTools.

**VDM-Regge**

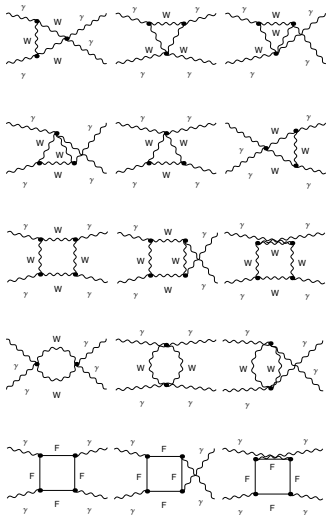
**WE ADD**

**2-gluon exch.**



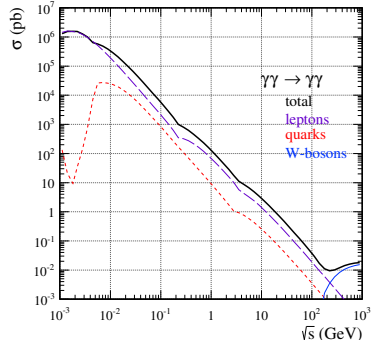
# BOXES

$$\gamma \gamma \rightarrow \gamma \gamma$$



Fermionic box LO QED - FormCalc.

The one-loop  $W$  box diagram - LoopTools.



We have compared our results with:

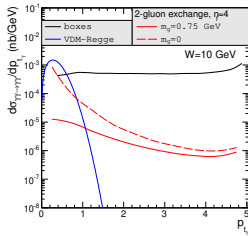
- Jikia et al. (1993),
- Bern et al. (2001),
- Bardin et al. (2009).

Bern et al. consider QCD and QED corrections (two-loop Feynman diagrams) to the one-loop fermionic contributions in the ultrarelativistic limit ( $\hat{s}, |\hat{t}|, |\hat{u}| \gg m_f^2$ ). The corrections are quite small numerically.

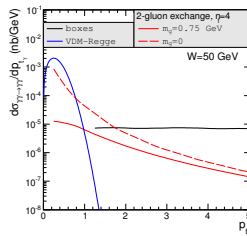
# EXPERIMENTAL IDENTIFICATION OF PROCESSES

- ✓ boxes
- ✓ VDM-Regge
- ✓ 2-gluon exchange

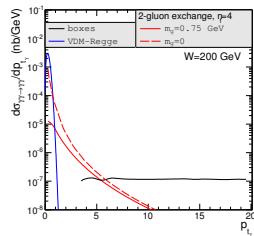
$W = 10 \text{ GeV}$



$W = 50 \text{ GeV}$



$W = 200 \text{ GeV}$



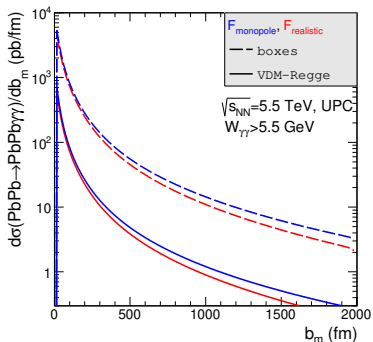
$\gamma - \gamma \text{ Collider?}$

# AA $\rightarrow$ AA $\gamma\gamma$ - FORM FACTOR

⇒ realistic

⇒ monopole

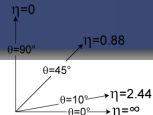
impact parameter



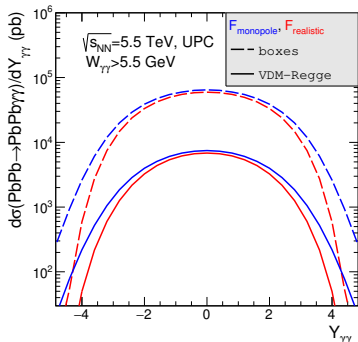
↑ theoretical distribution

$$\frac{\sigma_{\text{monopole}}}{\sigma_{\text{realistic}}}$$

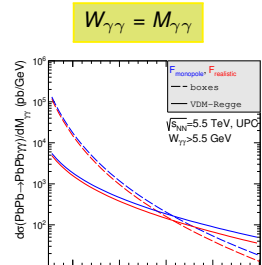
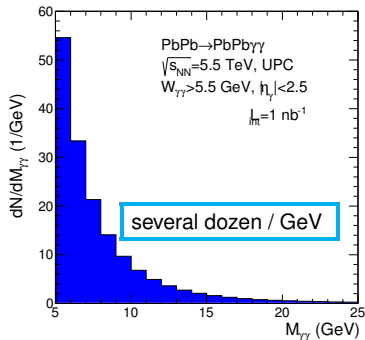
↗ for larger value of kinematical variables



$$Y_{\gamma\gamma} = \frac{1}{2} (y_{\gamma_1} + y_{\gamma_2})$$



$Y_{\gamma\gamma} \neq y_\gamma$



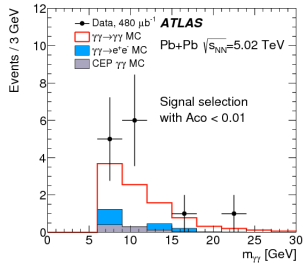
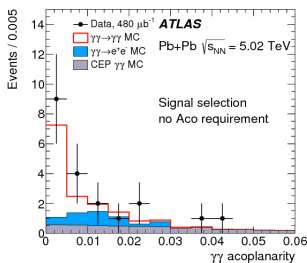
VDM-Regge dominates for  $W_{\gamma\gamma} > 30 \text{ GeV}$

$\sigma(\text{PbPb} \rightarrow \text{PbPb}\gamma\gamma) [\text{nb}]$  @ LHC ( $\sqrt{s_{NN}} = 5.5 \text{ TeV}$ ) & FCC ( $\sqrt{s_{NN}} = 39 \text{ TeV}$ )

|   | cuts   | boxes                  |                       | VDM-Regge              |                       |
|---|--|------------------------|-----------------------|------------------------|-----------------------|
|   |  | $F_{\text{realistic}}$ | $F_{\text{monopole}}$ | $F_{\text{realistic}}$ | $F_{\text{monopole}}$ |
| L | $W_{\gamma\gamma} > 5 \text{ GeV}$                               | 306                    | 349                   | 31                     | 36                    |
|   | $W_{\gamma\gamma} > 5 \text{ GeV}, p_{t,\gamma} > 2 \text{ GeV}$ | 159                    | 182                   | 7E-9                   | 8E-9                  |
|   | $E_\gamma > 3 \text{ GeV}$                                       | 16 692                 | 18 400                | 17                     | 18                    |
|   | $E_\gamma > 5 \text{ GeV}$                                       | 4 800                  | 5 450                 | 9                      | 611                   |
| H | $E_\gamma > 3 \text{ GeV},  y_\gamma  < 2.5$                     | 183                    | 210                   | 8E-2                   | 9E-2                  |
|   | $E_\gamma > 5 \text{ GeV},  y_\gamma  < 2.5$                     | 54                     | 61                    | 4E-4                   | 7E-4                  |
| C | $p_{t,\gamma} > 0.9 \text{ GeV},  y_\gamma  < 0.7$ (ALICE cuts)  | 107                    |                       |                        |                       |
|   | $p_{t,\gamma} > 5.5 \text{ GeV},  y_\gamma  < 2.5$ (CMS cuts)    | 10                     |                       |                        |                       |
| F | $W_{\gamma\gamma} > 5 \text{ GeV}$                               | 6 169                  |                       | 882                    |                       |
| C | $E_\gamma > 3 \text{ GeV}$                                       | 4 696 268              |                       | 574                    |                       |
| C |  |                        |                       |                        |                       |

# AA $\rightarrow$ AA $\gamma\gamma$ - ATLAS RESULTS

- ATLAS Collaboration (M. Aaboud et al.),  
Evidence for light-by-light scattering in heavy-ion collisions with the ATLAS detector at the LHC,  
Nature Phys. **13** (2017) 852  
Phys. Rev. Lett. **123** (2019) 052001



- ✗  $\gamma\gamma \rightarrow \gamma\gamma$  - Our results
- ✗ background:
  - ✓  $\gamma\gamma \rightarrow e^+e^-$
  - ✓  $gg \rightarrow \gamma\gamma$
  - ✓  $\gamma\gamma \rightarrow q\bar{q}$
- ✓ 13 events
- 59 events (2019)\*

$$\text{ATLAS} \Rightarrow \sigma = 70 \pm 20(\text{stat.}) \pm 17(\text{syst.}) \text{ nb}$$

$$(2019)^* \Rightarrow \sigma = 78 \pm 13(\text{stat.}) \pm 7(\text{syst.}) \pm 3(\text{lumi.}) \text{ nb}$$

$$\text{Our result} \Rightarrow \sigma = 51 \pm 0.02 \text{ nb}$$

# AA $\rightarrow$ AA $\gamma\gamma$ - CMS & ATLAS RESULTS - $M_{\gamma\gamma} > 5$ GEV

⇒ CMS Coll., Phys. Lett. **B797** (2019) 134826

- ✗  $E_{t,\gamma} > 2$  GeV
- ✗  $|\eta_\gamma| < 2.4$
- ✗  $M_{\gamma\gamma} > 5$  GeV
- ✗  $p_{t,\gamma\gamma} < 1$  GeV
- ✗  $A_{\text{Co}} < 0.01$

⇒ ATLAS Collaboration, JHEP 03 (2021) 243

- ✗  $E_{t,\gamma} > 2.5$  GeV
- ✗  $|\eta_\gamma| < 2.4$
- ✗  $M_{\gamma\gamma} > 5$  GeV
- ✗  $p_{t,\gamma\gamma} < 1$  GeV
- ✗  $A_{\text{Co}} < 0.01$

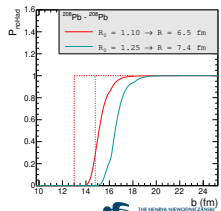
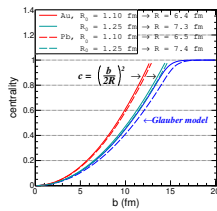
| Collaboration     | $\sigma$ nb                                     | Experiment                |                             | Theory                    | Glauber model<br>$\sigma(b = 20\text{fm})$ |
|-------------------|---|---------------------------|-----------------------------|---------------------------|--|
|                   |   | $\sigma(b = 13\text{fm})$ | $\sigma(b = 14.8\text{fm})$ | $R = R_0 A^{\frac{1}{3}}$ |  |
| ATLAS (2018 data) | $78 \pm 13(\text{stat.}) \pm 7(\text{syst.})$   | 52                        | 50                          |                           | 45   |
| ATLAS (2015+2018) | $120 \pm 17(\text{stat.}) \pm 13(\text{syst.})$ | 82                        | 80                          |                           | 71   |
| CMS (2015)        | $120 \pm 46(\text{stat.}) \pm 28(\text{syst.})$ | 105                       | 103                         |                           | 92   |

UPC  $\rightarrow b_{\min} > 2 \times R$

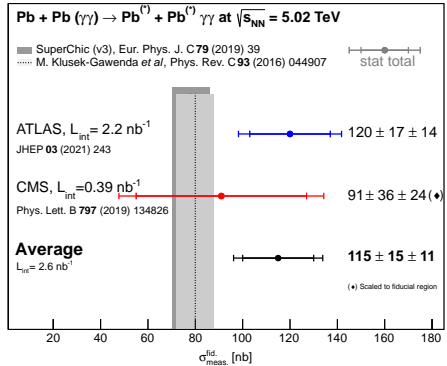
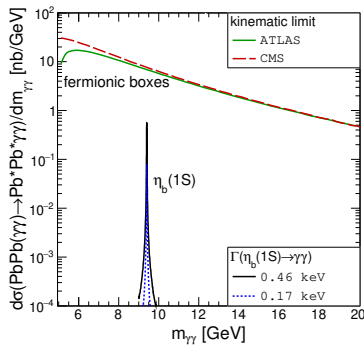
14 FM

$$\rightarrow P_{\text{NoHadronic}}(\vec{b}) = \exp(-\sigma_{NN} T_{AA}(\vec{b}))$$

|                    |        |
|--------------------|--------|
| centrality [%]     | 100    |
| nucleus and radius | b (fm) |
| Pb, $R = 6.5$ fm   | 13.0   |
| Pb, $R = 7.4$ fm   | 14.8   |
| Pb Pb, Glauber     | 20.0   |



# 2022 RESULTS

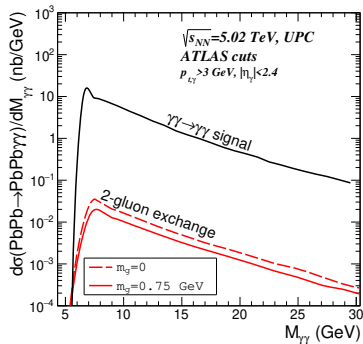


This result paves the way for combining existing or forthcoming measurements using LHC heavy-ion collisions and provides, within the studied phase space region, an additional experimental input to the comparison with state-of-the-art predictions from quantum electrodynamics.

- ➡ The European Union's Horizon 2020 research and innovation program under the STRONG-2020,  
G. K. Krintiras, I. Grabowska-Bold, M. Klusek-Gawenda and É. Chapon R. Chudasama and R. Granier de Cassagnac,  
*arXiv:2204.02845 [hep-ph]*;  
Light-by-light scattering cross-section measurements at LHC

# HIGHER ORDER PROCESSES..?

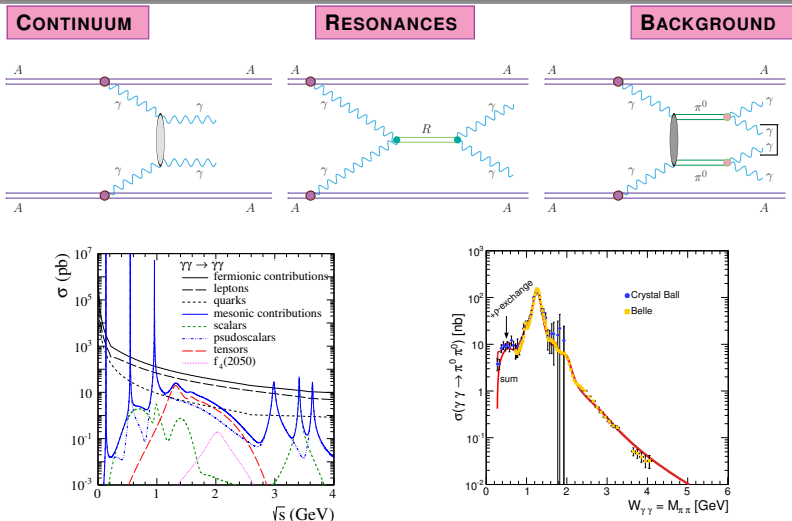
$\gamma\gamma$  invariant mass



Coherent sum of both processes...?

Pionic boxes...?

# AA $\rightarrow$ AA $\gamma\gamma$ FOR $M_{\gamma\gamma} < 5$ GEV ?



- » P. Lebiedowicz, A. Szczurek, *Phys. Lett. B772* (2017) 330,  
The role of meson exchanges in light-by-light scattering

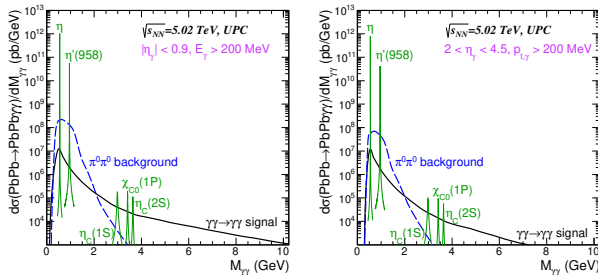
- » M. K-G, A. Szczurek, *Phys. Rev. C87* (2013) 054908;  
 $\pi^+\pi^-$  and  $\pi^0\pi^0$  pair production in photon-photon and in ultraperipheral ultrarelativistic heavy-ion collisions

## UPC OF AA...

ALICE cuts

- boxes
- bkg
- mesons

LHCb cuts

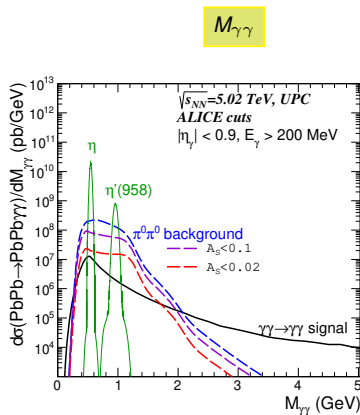
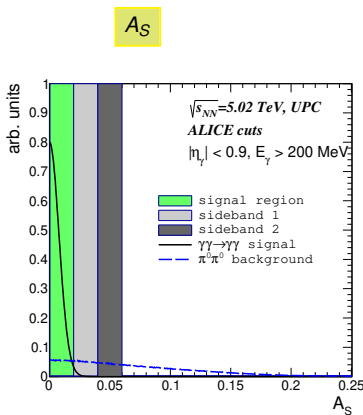


Total nuclear cross section [nb]

| Energy           | $W_{\gamma\gamma} = (0 - 2)$ GeV |         | $W_{\gamma\gamma} > 2$ GeV |      |
|------------------|----------------------------------|---------|----------------------------|------|
|                  | Fiducial region                  | ALICE   | LHCb                       | LHCb |
| Boxes            |                                  | 4 890   | 3 818                      | 146  |
| $\pi^0\pi^0$ bkg |                                  | 135 300 | 40 866                     | 24   |
| $\eta$           |                                  | 722 573 | 568 499                    |      |
| $\eta'(958)$     |                                  | 54 241  | 40 482                     |      |
| $\eta_c(1S)$     |                                  |         |                            | 9    |
| $\chi_{c0}(1P)$  |                                  |         |                            | 4    |
| $\eta_c(2S)$     |                                  |         |                            | 1    |

## EXPERIMENTAL RESOLUTION &amp; SCALAR ASYMMETRY &amp; "UNWANTED" BKG

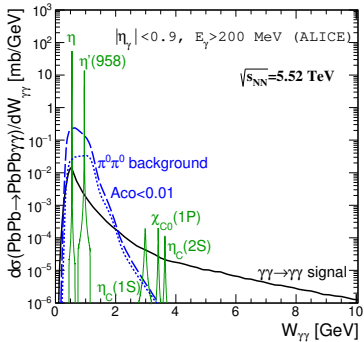
$$A_S = \left| \frac{|\vec{p}_T(1)| - |\vec{p}_T(2)|}{|\vec{p}_T(1)| + |\vec{p}_T(2)|} \right|$$



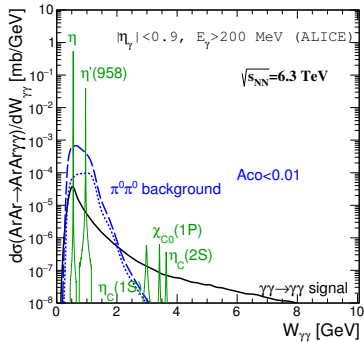
80% of the signal events at  $A_S < 0.02$

# AA $\rightarrow$ AA $\gamma\gamma$ @ MIDRAPIDITY

$^{208}\text{Pb}^{82+} + ^{208}\text{Pb}^{82+}$



$^{40}\text{Ar}^{18+} + ^{40}\text{Ar}^{18+}$



$$\sqrt{s_{NN}} = \sqrt{\frac{Z_1 Z_2}{A_1 A_2}} \sqrt{s_{pp}}$$

$$\sigma_{tot} \propto (Z_{Pb}/Z_{Ar})^4 \approx 430$$

Run 5:  $L_{int}^{\text{Ar-Ar}} = (3 - 8.8) \text{ pb} \rightarrow 1460 - 4280$  signal events ( $W_{\gamma\gamma} > 2$  GeV)



# AA $\rightarrow$ AA $\gamma\gamma$ @ FORWARD REGION ?

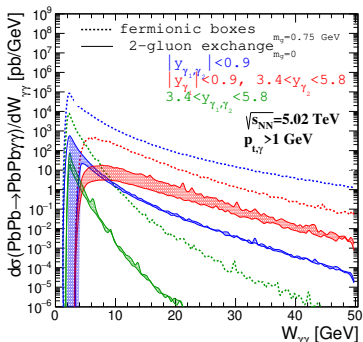
✓ ALICE Collaboration,

*Letter of Intent: A Forward Calorimeter (FoCal) in the ALICE experiment,  
CERN-LHCC-2020-009*

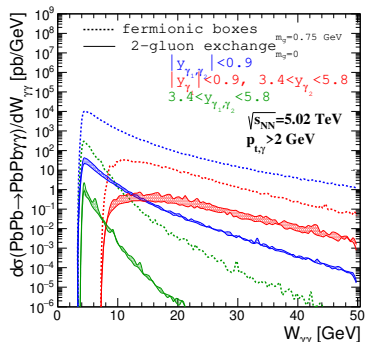
FOCAL →  $3.4 < \eta < 5.8$

The forward electromagnetic and hadronic calorimeter is an upgrade to the ALICE experiment, to be installed during LS3 for data-taking in 2027–2029 at the LHC.

$p_{t,\gamma} > 1 \text{ GeV}$



$p_{t,\gamma} > 2 \text{ GeV}$



Boxes & 2-gluon exchange (with effective gluon mass)

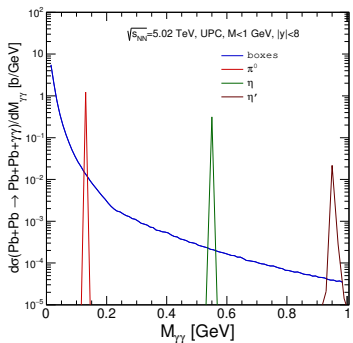


19736

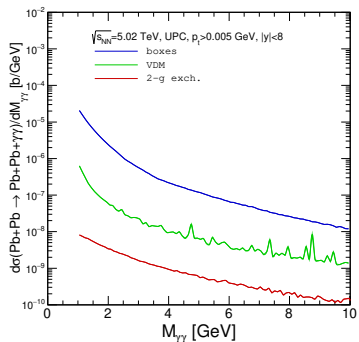
# AA $\rightarrow$ AA $\gamma\gamma$ @ LOW $p_t$ REGION ?

$p_{t,\gamma} > 5 \text{ MeV}$

$M_{\gamma\gamma} < 1 \text{ GeV}$

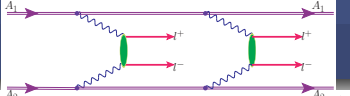


$M_{\gamma\gamma} > 1 \text{ GeV}$



ALICE3 - new opportunities

# FOUR-LEPTON PRODUCTION



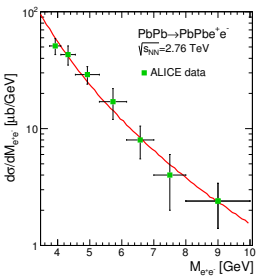
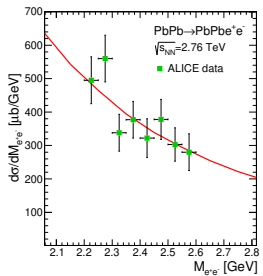
$$\frac{d\sigma_{A_1 A_2 \rightarrow A_1 A_2 (\ell^+ \ell^-)(\ell^+ \ell^-)}}{dy_{\ell^+}^I dy_{\ell^-}^I dy_{\ell^+}^{II} dy_{\ell^-}^{II}} = \frac{1}{2} \int \left( \frac{dP_{\gamma\gamma \rightarrow \ell^+ \ell^-}^I(b, y_{\ell^+}^I, y_{\ell^-}^I; p_{t,\ell})}{dy_{\ell^+}^I dy_{\ell^-}^I} \times \frac{dP_{\gamma\gamma \rightarrow \ell^+ \ell^-}^{II}(b, y_{\ell^+}^{II}, y_{\ell^-}^{II}; p_{t,\ell})}{dy_{\ell^+}^{II} dy_{\ell^-}^{II}} \right) \times 2\pi b db$$

$$P_{\gamma\gamma \rightarrow \ell^+ \ell^-}(b; y_{\ell^+}, y_{\ell^-}, p_{t,\ell}) = \int N(\omega_1, \mathbf{b}_1) N(\omega_2, \mathbf{b}_2) S_{abs}^2(\mathbf{b}) \times \frac{d\sigma_{\gamma\gamma \rightarrow \ell_1 \ell_2}(W_{\gamma\gamma})}{d\cos\theta} d\bar{b}_x d\bar{b}_y \frac{W_{\gamma\gamma}}{2} dW_{\gamma\gamma} dY_{\ell_1 \ell_2}$$

$2.2 \text{ GeV} < M_{ee} < 2.6 \text{ GeV}$

$|y_e| < 0.9$

$3.7 \text{ GeV} < M_{ee} < 10 \text{ GeV}$

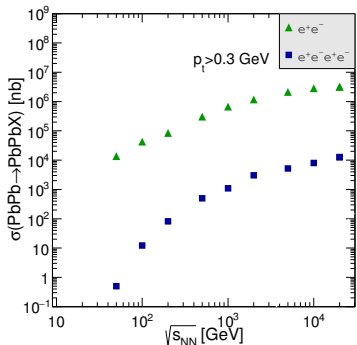


Good description of single pair production  $\Rightarrow$  two  $e^+e^-$  pair production

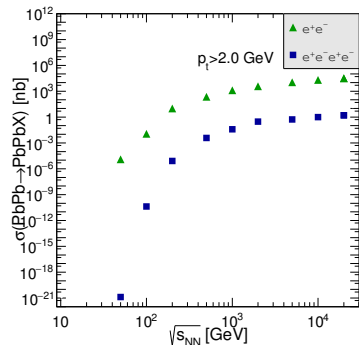
$$AA \rightarrow AAe^+e^- \text{ & } AA \rightarrow AAe^+e^-e^+e^-$$

**Single  $e^+e^-$  pair production  
vs.  
double scattering production of two  $e^+e^-$  pairs**

$p_t > 0.3 \text{ GeV}$

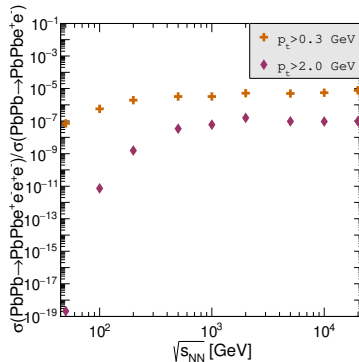


$p_t > 2.0 \text{ GeV}$



$$AA \rightarrow AAe^+e^- \text{ & } AA \rightarrow AAe^+e^-e^+e^-$$

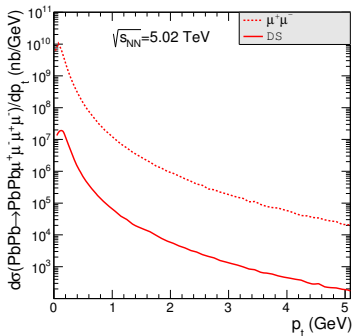
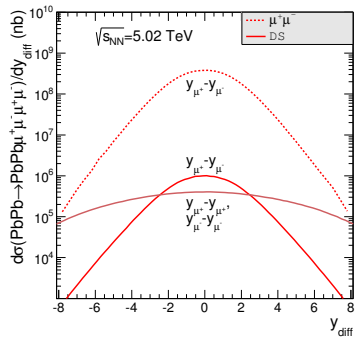
$$\frac{\sigma_{AA \rightarrow AAe^+e^-e^+e^-}}{\sigma_{AA \rightarrow AAe^+e^-}}$$



Ratio depends on  $\sqrt{s_{NN}}$  and  $p_{t,min}$

$$AA \rightarrow AA\mu^+\mu^- \text{ & } AA \rightarrow AA\mu^+\mu^-\mu^+\mu^-$$

**Single  $\mu^+\mu^-$  pair production  
vs.  
double scattering production of two  $\mu^+\mu^-$  pairs**

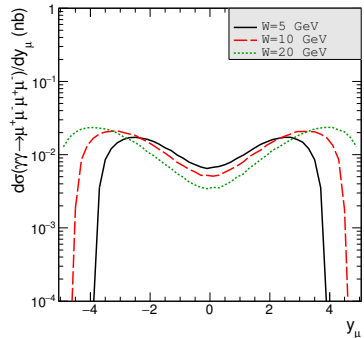
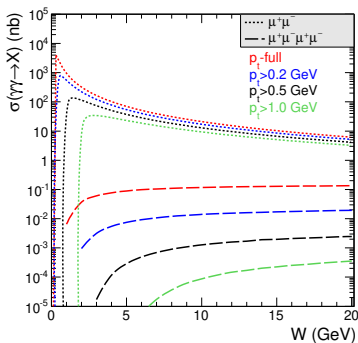
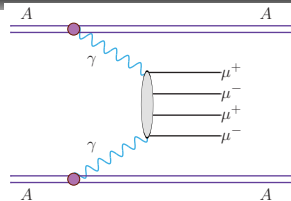
 $p_{t,\mu}$  $y_{diff}$ 

Like for electron-positron production:  $\sigma_{\mu^+\mu^-} \simeq 1000 \times \sigma_{\mu^+\mu^-\mu^+\mu^-}$

# $\gamma\gamma \rightarrow \mu^+\mu^-\mu^+\mu^-$ - SINGLE SCATTERING

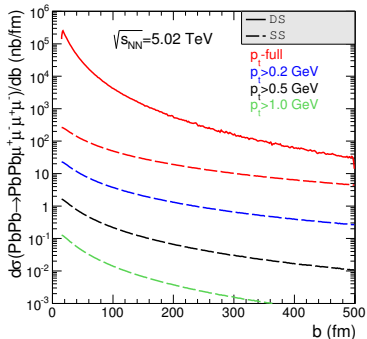


KATIE- an event generator that is specially designed to deal with initial states that have an explicit transverse momentum dependence but can also deal with on-shell initial states. KATIE is a parton-level generator for hadron scattering but requires only a few adjustments to deal with photon scattering.

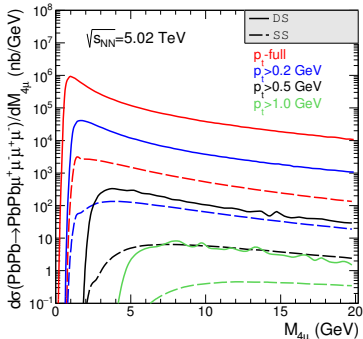


$$\text{AA} \rightarrow \text{AA} \mu^+ \mu^- \mu^+ \mu^-$$

impact parameter



↑ purely theoretical distribution

 $W_{\gamma\gamma} = M_{4\mu}$ 

↑ DS dominates

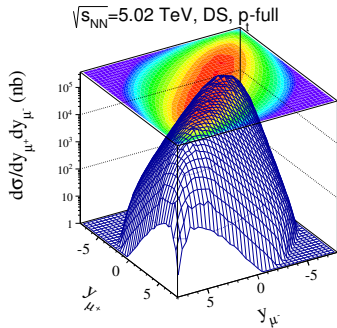
It is difficult to isolate range of SS domination

\*DS - double-scattering mechanism

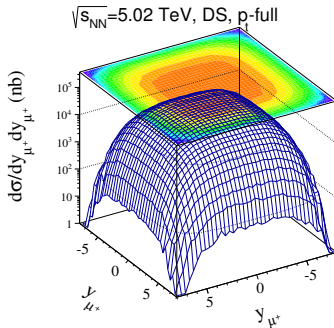
\*SS - a NEW single-scattering mechanism

$\text{AA} \rightarrow \text{AA} \mu^+ \mu^- \mu^+ \mu^-$

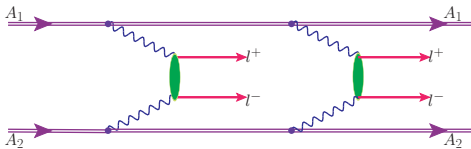
$y_{\mu^+}, y_{\mu^-}$



$y_{\mu^\pm}, y_{\mu^\pm}$



$p_{t,\mu^+} \simeq p_{t,\mu^-} \Rightarrow$  construction of similar distributions by ALICE or CMS?



The number of counts for  $L_{int} = 1 \text{ nb}^{-1}$

| $(4\mu), \sqrt{s_{NN}} = 5.02 \text{ TeV}$ |         | $(4e), \sqrt{s_{NN}} = 5.5 \text{ TeV}$ |     |
|--|---------|---|-----|
| experimental cuts                          | N       | experimental cuts                       | N   |
| $ y_i  < 2.5, p_t > 0.5 \text{ GeV}$       | 815     | $ y_i  < 2.5, p_t > 0.5 \text{ GeV}$    | 235 |
| $ y_i  < 2.5, p_t > 1.0 \text{ GeV}$       | 53      | $ y_i  < 2.5, p_t > 1.0 \text{ GeV}$    | 10  |
| $ y_i  < 0.9, p_t > 0.5 \text{ GeV}$       | 31      | $ y_i  < 1.0, p_t > 0.2 \text{ GeV}$    | 649 |
| $ y_i  < 0.9, p_t > 1.0 \text{ GeV}$       | 2       | $ y_i  < 1.0, p_t > 1.0 \text{ GeV}$    | 1   |
| $ y_i  < 2.4, p_t > 4.0 \text{ GeV}$       | $\ll 1$ |   |     |

CMS and ALICE  $\Rightarrow p_{t,\text{cut}} = 1 \text{ GeV}$

ALICE  $\Rightarrow p_{t,\text{cut}} = 0.2 \text{ GeV}$

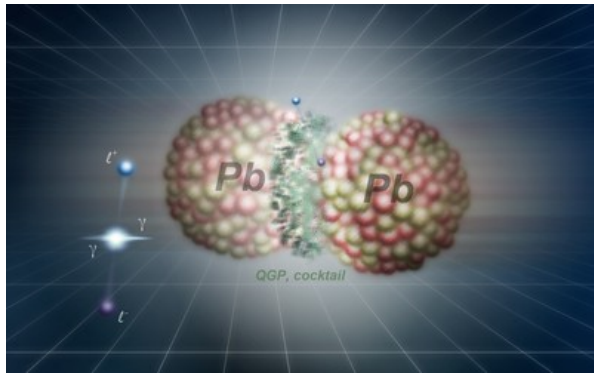
ATLAS  $\Rightarrow p_{t,\text{cut}} = 4 \text{ GeV}$

## Potential background

$$\downarrow \sqrt{s_{NN}} = 5.5 \text{ TeV}, |y| < 4.9$$

| Reaction                                    | $p_{t,\text{min}} = 0.3 \text{ GeV}$ | $p_{t,\text{min}} = 0.5 \text{ GeV}$ |
|---|--------------------------------------|--------------------------------------|
| $PbPb \rightarrow PbPb\pi^+\pi^-\pi^+\pi^-$ | 2.954 mb                             | 8.862 $\mu\text{b}$                  |
| $PbPb \rightarrow PbPbe^+e^-e^+e^-$         | 7.447 $\mu\text{b}$                  | 0.704 $\mu\text{b}$                  |

# SEMICENTRAL HEAVY-ION COLLISIONS



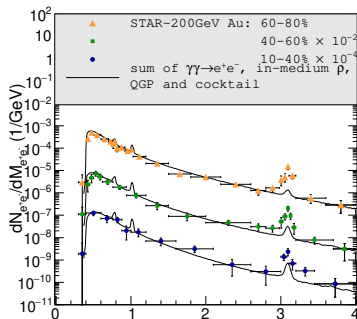
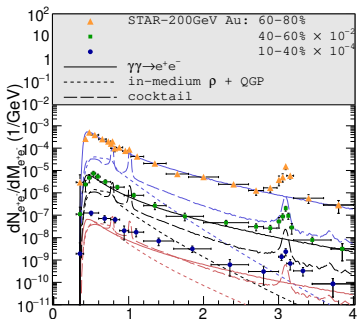
- From ultraperipheral to semicentral collisions → dilepton sources
  - $\gamma\gamma$  fusion mechanism
- Invariant mass
  - SPS (NA60 data)
  - RHIC (STAR data)
  - LHC (ALICE data)
- Low- $P_T$  dilepton spectra
  - RHIC (STAR data)
  - LHC (ALICE data)
- Acoplanarity
  - LHC (ATLAS data)

## DIELECTRON INVARIANT-MASS SPECTRA - RHIC

 $p_t > 0.2 \text{ GeV}$  $|\eta_e| < 1$  $|y_{e^+ e^-}| < 1$ 

- ✓  $\gamma\gamma$ -fusion
- ✓ thermal radiation
- ✓ hadronic cocktail

3 centrality classes



The coherent emission dominates for the two peripheral samples

and is comparable to the cocktail and thermal radiation yields in semi-central collisions.

**EPA in the impact parameter space - the pair transverse momentum  $P_T^{\ell^+\ell^-}$  is neglected**

$$\sigma_{A_1 A_2 \rightarrow A_1 A_2 \ell^+ \ell^-} = \int N(\omega_1, \mathbf{b}_1) N(\omega_2, \mathbf{b}_2) \delta^{(2)}(\mathbf{b} - \mathbf{b}_1 - \mathbf{b}_2) \int d^2 \mathbf{b}_1 d^2 \mathbf{b}_2 d^2 \mathbf{b} dy_{\ell^+} dy_{\ell^-} dp_{t,\ell}^2 \frac{d\sigma(\gamma\gamma \rightarrow \ell^+ \ell^-; \hat{s})}{d(-\hat{t})}$$

⇒  $k_t$ -factorization

$$\frac{dN_{II}}{d^2 \mathbf{P}_T^{\ell^+ \ell^-}} = \int \frac{d\omega_1}{\omega_1} \frac{d\omega_2}{\omega_2} d^2 \mathbf{q}_{1t} d^2 \mathbf{q}_{2t} \frac{dN(\omega_1, q_{1t}^2)}{d^2 \mathbf{q}_{1t}} \frac{dN(\omega_2, q_{2t}^2)}{d^2 \mathbf{q}_{2t}} \delta^{(2)}(\mathbf{q}_{1t} + \mathbf{q}_{2t} - \mathbf{P}_T^{\ell^+ \ell^-}) \hat{\sigma}(\gamma\gamma \rightarrow \ell^+ \ell^-) \Big|_{\text{cuts}},$$

⇒ Exact calculation

$$\begin{aligned} \frac{d\sigma[C]}{d^2 \mathbf{P}_T^{\ell^+ \ell^-}} &= \int \frac{d^2 \mathbf{Q}}{2\pi} w(Q; b_{\max}, b_{\min}) \int \frac{d^2 \mathbf{q}_1}{\pi} \frac{d^2 \mathbf{q}_2}{\pi} \delta^{(2)}(\mathbf{P}_T^{\ell^+ \ell^-} - \mathbf{q}_1 - \mathbf{q}_2) \int \frac{d\omega_1}{\omega_1} \frac{d\omega_2}{\omega_2} \\ &\times E_i\left(\omega_1, \mathbf{q}_1 + \frac{\mathbf{Q}}{2}\right) E_j^*\left(\omega_1, \mathbf{q}_1 - \frac{\mathbf{Q}}{2}\right) E_k\left(\omega_2, \mathbf{q}_2 - \frac{\mathbf{Q}}{2}\right) E_l^*\left(\omega_2, \mathbf{q}_2 + \frac{\mathbf{Q}}{2}\right) \frac{1}{2\hat{s}} \sum_{\lambda \bar{\lambda}} M_{ik}^{\lambda \bar{\lambda}} M_{jl}^{\lambda \bar{\lambda} \dagger} d\Phi(\ell^+ \ell^-). \end{aligned}$$

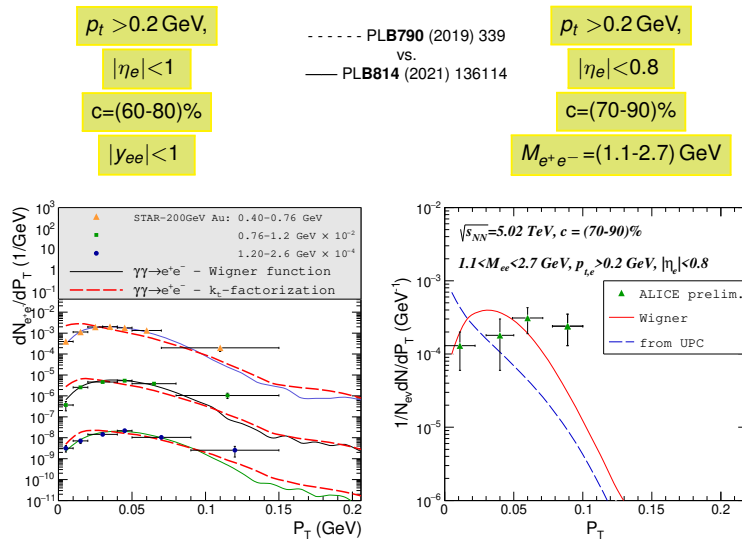
The factorization formula is written in terms of the Wigner function:

$$N_{ij}(\omega, \mathbf{b}, \mathbf{q}) = \int \frac{d^2 \mathbf{Q}}{(2\pi)^2} \exp[-i\mathbf{b}\mathbf{Q}] E_i\left(\omega, \mathbf{q} + \frac{\mathbf{Q}}{2}\right) E_j^*\left(\omega, \mathbf{q} - \frac{\mathbf{Q}}{2}\right) = \int d^2 \mathbf{s} \exp[i\mathbf{qs}] E_i\left(\omega, \mathbf{b} + \frac{\mathbf{s}}{2}\right) E_j^*\left(\omega, \mathbf{b} - \frac{\mathbf{s}}{2}\right),$$

$$N(\omega, \mathbf{q}) = \delta_{ij} \int d^2 \mathbf{b} N_{ij}(\omega, \mathbf{b}, \mathbf{q}) = \delta_{ij} E_i(\omega, \mathbf{q}) E_j^*(\omega, \mathbf{q}) = |\mathbf{E}(\omega, \mathbf{q})|^2,$$

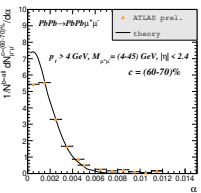
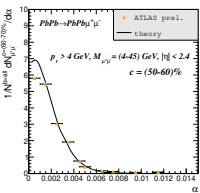
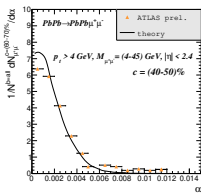
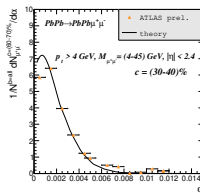
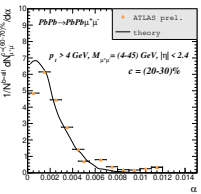
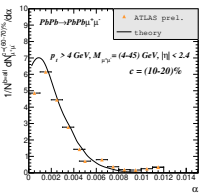
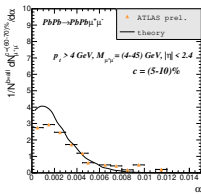
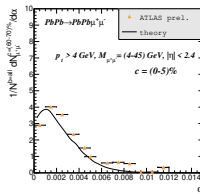
$$N(\omega, \mathbf{b}) = \delta_{ij} \int \frac{d^2 \mathbf{q}}{(2\pi)^2} N_{ij}(\omega, \mathbf{b}, \mathbf{q}) = \delta_{ij} E_i(\omega, \mathbf{b}) E_j^*(\omega, \mathbf{b}) = |\mathbf{E}(\omega, \mathbf{b})|^2.$$

# PAIR TRANSVERSE MOMENTUM - RHIC & LHC



Small correction to the STAR description & much better situation for LHC

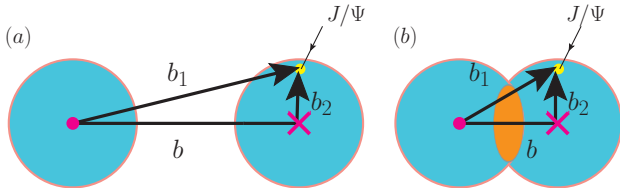
# ACOPLANARITY - ATLAS DATA



A successful description of ATLAS data by  $\gamma\gamma$ -fusion alone

A correct normalization and shape of the distributions

# CHARMONIUM PHOTOPRODUCTION

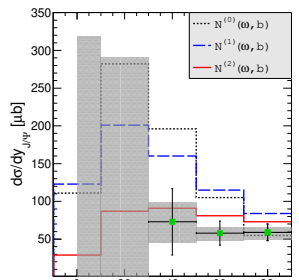


**The inclusion of the absorption effect by modifying effective photon fluxes in the impact parameter space.**

$$N^{(1)}(\omega_1, b) = \int N(\omega_1, b_1) \frac{\theta(R_A - (|\mathbf{b}_1 - \mathbf{b}|))}{\pi R_A^2} d^2 b_1$$

$$N^{(2)}(\omega_1, b) = \int N(\omega_1, b_1) \frac{\theta(R_A - (|\mathbf{b}_1 - \mathbf{b}|))(b_1 - R_A)}{\pi R_A^2} d^2 b_1$$

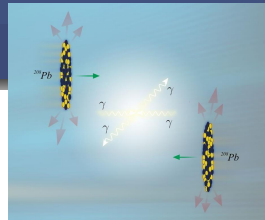
A successful description of ALICE data



# CONCLUSION

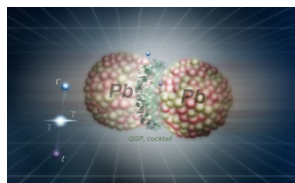
- EPA in **the impact parameter space**
- Ultraperipheral & semicentral heavy-ion collisions
- Fourier transform of the charge distribution
- Multidimensional integrals → differential cross section
- **Description** of experimental data for UPC and semicentral events
  - STAR -  $e^+e^-$ ,  $\pi^+\pi^-\pi^+\pi^-$
  - ATLAS -  $\gamma\gamma$ ,  $\mu^+\mu^-$
  - ALICE -  $e^+e^-$ ,  $J/\psi$
  - CMS -  $\gamma\gamma$
- **Predictions** focused on experimental acceptance
  - $\mu^+\mu^-\mu^+\mu^-$  - single & double scattering
  - $e^+e^-e^+e^-$  - double scattering
  - $p\bar{p}$
  - $\pi^+\pi^-$  &  $\pi^0\pi^0$
  - $\gamma\gamma$  for  $M_{\gamma\gamma} < 5 \text{ GeV}$
- Collaboration - theoreticians and experimenters
- Future - study of processes in low  $p_t$  (ALICE3)

Thank you



**Photon collisions: Photonic billiards might be the newest game!**, EurekAlert!

Ultraperipheral collisions of lead nuclei at the LHC accelerator can lead to elastic collisions of photons with photons.



**Creation without contact in the collisions of lead and gold nuclei**, EurekAlert!

Semicentral or central collisions of lead nuclei in the LHC produce QGP and a cocktail with contributions of other particles. Simultaneously, clouds of photons surrounding the nuclei collide, resulting in the creation of  $\ell^+\ell^-$  pairs within the plasma and cocktail, and in the space around the nuclei.